JSEE Vol. 27, No. 1, 2025 DOI: 10.48303/jsee.2024.2038378.1119

***Research Paper***

# Collapse Mechanism Investigation of Mass-Isolated Systems

***Saeid Saharkhizan[1*] and Mansour Ziyaeifar[2]***

1. Ph.D. Candidate, Structural Engineering Research Center, International Institute of Earthquake Engineering and Seismology (IIEES), Tehran, Iran, *Corresponding Author email: saeid.saharkhizan@stu.iiees.ac.ir
2. Associate Professor, Structural Engineering Research Center, International Institute of Earthquake Engineering and Seismology (IIEES), Tehran, Iran

**Received:** 14/08/2024
**Revised:** 22/08/2024
**Accepted:** 24/08/2024

**Keywords:**
Mass-isolation; Multi-phase behavior; Damping amplification; Impact; Collapse probability

## ABSTRACT

Rare earthquakes cause heavy damages to building structures. Design of structures using yield mechanisms that provide extra resources to ensure structural stability for intensity higher than the design-based earthquake (DBE), can be considered as a reasonable technique to reduce the collapse probability. In this regard, the design of a mass-isolated structural system with a multi-phase seismic behavior as a reliable lateral load-bearing system has been investigated. In this type of configuration, by separating the mass from the stiffness of the system in the vertical direction, the structural system is transformed into two subsystems (soft and stiff), which can be utilized as an effective damping amplification technique by using an appropriate energy dissipation mechanism between these two parts. Furthermore, it can be used as an efficient seismic rehabilitation method for non-code-confirmed structures. In this study, in addition to performing parametric studies to determine the optimal damping coefficient, the impact and ultimate collapse mechanism of the system have been simulated and investigated numerically. The results of nonlinear time history analysis indicate that the mass-isolation technique can efficaciously improve the seismic performance of buildings compared to conventional structural systems due to the multi-phase seismic behavior.

How to cite the article:
Saharkhizan, S., & Ziyaeifar, M. (2025). Collapse Mechanism Investigation of Mass-Isolated Systems. *Journal of Seismology and Earthquake Engineering*, *27*(1), 73-87. doi: 10.48303/jsee.2024.2038378.1119

## 1. Introduction

Earthquakes with intensity higher than the design-based level (DBE) up to the maximum considered earthquake (MCE) and greater may cause extensive damage to building structures. In the ductility-based seismic design approach, the only available mechanism to prevent collapse in severe earthquakes is the development of inelastic action in structural components. Although a large amount of input energy is dissipated by this method, this causes large displacements and considerable damages to structural and non-structural elements, which increases the costs of repair, replacement, or retrofitting after the earthquake. In addition, the intensification of the P-Δ effect increases the risk of global instability.

The recent devastating earthquake in Turkiye (2023 Turkiye-Syria earthquake), in confirmation of this claim, revealed that perhaps our estimations about seismic risk for case of rare earthquakes are not accurate enough, and therefore relying only on the ductility of base system for earthquakes higher than the design level intensity cannot guarantee the appropriate performance of buildings and ensure their safety objectives. The question that arises here is, whether such levels of extensive damages in the building should be con-sidered normal? Are there any methods for severe earthquakes to delay the collapse of the structure by relying on mechanisms other than structural ductility (for example, extra resources of ductility, stiffness and strength) while guaranteeing the performance targets and enhancing the reliability of the system?

Vibration isolation through the base isolation technique is one of the effective methods for reducing the dynamic response of structures. This isolation method, while dominating the first mode of vibration (minimizing the effects of higher modes), causes a significant increase in the natural period of vibration and as a result, reduces the seismic demand in the structural components (Cheng, 2008). The application of this technique is limited by increasing the height of the building for two main reasons: First, due to the increase in the natural period of the building, and second, the problems caused by the large weight of the building and its restrictive effects on the design and construction of a desired isolator relating to the technical issues. Consequently, for tall buildings, the damping enhancement approach is employed. However, for this type of structure, damper efficiency is diminished due to the constraints in inter-story drift ratio (given the higher importance of tall buildings). Therefore, to achive high damping ratios, it is necessary to utilize dampers with higher capacity and this issue affects the economy of the project.

In recent years, more attention has been paid to modern methods of seismic design, and in this regard, the concept of mass isolation has been proposed as a rational vibration isolation method for mid to high-rise buildings. The main philosophy of this method is to use two mechanisms of flexibility and damping enhancement in the structure to improve performance levels without extensive use of structural ductility. In fact, due to the importance of the mass parameter in the earthquake input energy, instead of isolating the entire mass and stiffness of the building from the ground (like the base isolation technique), it will be appropriate to isolate only the horizontal component of the building mass from its stiffness by using an isolator layer distributed at the height of the structure (Ziaeifar, 2002). This method converts a structural system into two subsystems (mass and stiffness) and, as a result, causes a significant difference in the natural frequency of vibration of the subsystems.

Using appropriate energy dissipation devices between two parts is a suitable technique for the seismic design of struct-ure by obtaining a multi-phase behavior and increasing its damping ratio (Figure 1a).

The requirement for the proper performance of this type of structural configuration is the occurrence of relative displacement and velocity with a considerable range between two subsystems. If these conditions are met, dampers with significantly lower capacity (which are not necessarily used in all stories) will be able to dissipate a large amount of the input seismic energy and consequently improve the safety. Furthermore, as illustrated in Figure (1b), increasing the natural period of vibration of the mass substructure (the main part of the system) reduces the seismic demand in this part and consequently improves the seismic performance of the system.

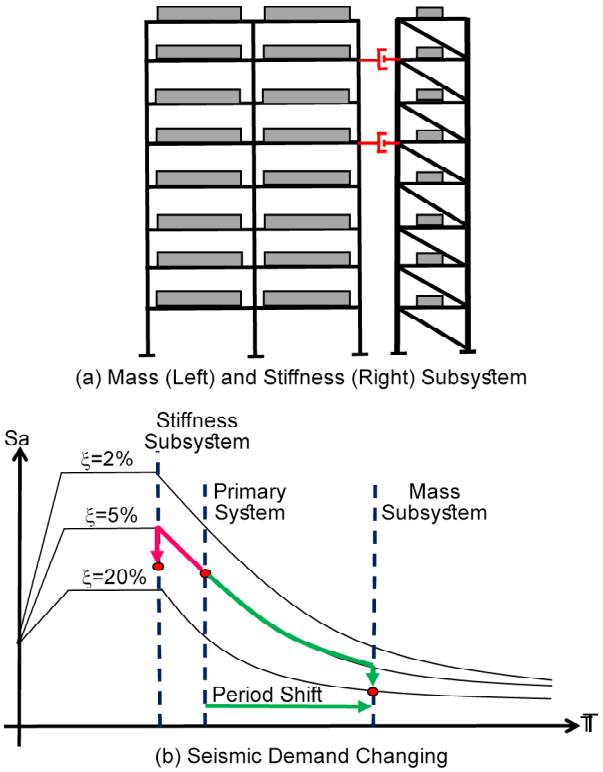


**Figure 1.** Mass isolation concept.

In 2012, Ziyaeifar et al. proposed a two-mass model to investigate the dynamic behavior of mass-isolated structures (Ziyaeifar et al., 2011). The proposed model was a development of Maxwell's damper model, and the non-classical eigenvalue analysis highlighted the importance of energy dissipation elements in determining the system's dynamic characteristics. Moreover, the results of the time integration analysis indicated that using a viscous damper between two subsystems can decrease the displacement response of the system compared to the initial state of the connected structure (non-isolated structure) both in the controlled and uncontrolled states. In 2019, Boujary and Ziyaeifar (2019a) proposed a method for designing a mass subsystem based on consideration of stability constraints. Recently, the concept of mass isolation in suspended isolated system forms has been explored, demonstrating its effectiveness in dynamic response suppression through numerical and experimental validation (Nakamura et al., 2010; Ye & Wu, 2019; Du et al., 2022). In 2024, Saharkhizan and Ziyaeifar investigated the seismic behavior of mass-isolated system under severe earthquakes. The results from stability and nonlinear analyses indicated that this structural typology could effectively enhance seismic performance compared to conventional structures, owing to its multi-phase seismic behavior (Saharkhizan & Ziyaeifar, 2024).

The fundamental idea of mass-isolation has been studied conceptually in recent years; however, by now, comprehensive studies have not been conducted to investigate the seismic behavior of this structural typology under severe earthquakes and the determination of failure modes and collapse mechanisms. The main question is whether this structural topology can offer a performance advantage over conventional systems by generating multi-phase behavior and enhancing the system's safety by reducing the probability of collapse. In this study, an in-depth investigation of the issue will be conducted.

## 2. Design Concept

It is essential that the mass subsystem's contribution to the system's stiffness is minimal while to the system's mass is maximized. Additionally, the stiffness subsystem should contribute maximally to the structure's stiffness and minimally to the system's mass. However, to what extent are these degrees of flexibility and stiffness practical in such a way that both the desired seismic performance of the system is satisfied and the system is economically justified?

### *2.1. Stability Consideration*

Reducing the lateral stiffness of the system increases its natural period of vibration, thereby decreases the seismic demands on structural components (Figure 1b). Since most of the building mass is supported by the mass substructure, flexibility enhancement will improve the design's efficiency and economy, as long as the mass subsystem be able to withstand gravity and lateral loads up to the desired performance level. Conversely, excessive reduction of the lateral stiffness in the mass subsystem may trigger non-ductile failure modes, such as buckling (both locally and globally), which significantly impacts the system's seismic performance targets. This issue complicates the securance of the system's stability by increasing the structure's height and intensifying the P-Δ effect.

The appropriate seismic design approach for this type of structural configuration will be performance-based and proportional to the lateral displacement capacity of subsystems (PEER, 2017). Considering this issue, since the mass subsystem will be designed in its softest form (minimum stiffness required for stability criteria), this reduction in stiffness exceeds the typical limits of conventional code-compliant structures, thereby increases the probability of instability. Consequently, limiting the lateral displacement of the mass subsystem and ensuring its stability will be the primary controlling and influential parameter in the design process. Therefore, it is essential to identify the softest possible structure for the mass subsystem that can withstand the anticipated threshold of lateral displacement without collapsing. This necessitates a logical relationship between the stability characteristics of the mass substructure (for instance, the stability index θ, or the critical buckling load factor, λ) and the load intensity characteristics (such as the spectral acceleration $S_a$). For this purpose, previous studies have aimed to estimate the minimum design base shear required to ensure the stability of the mass subsystem up to the expected lateral displacement (Bernal, 1992, 1998; Boujary & Ziyaeifar, 2019a-b). Equations (1) to (5) provide the details of the relevant calculations.

$$T = 2\pi\sqrt{(2N+1)/g\lambda_0} \tag{1}$$

$$S(\delta;\theta) = \frac{V}{M} = \frac{S_e}{(1-\theta)} \times \left(0.037\delta^3 - 0.444\delta^2 + (1.778-\theta)\delta - 0.37\right) \tag{2}$$

$$1 < \delta = \frac{\Delta}{\Delta_e} < \beta\Omega \tag{3}$$

$$\Delta_e = \frac{\Delta_y}{\Omega} \tag{4}$$

$$\beta \cong \frac{P_u}{P_s} = \frac{1.2D+1.6L}{D+0.2L} \tag{5}$$

where $N$ is the number of stories, $\lambda_0$ is critical buckling load coefficient, $S$ is the lateral load-bearing capacity of the structure normalized to the total mass of the structure, $S_e$ is the normalized lateral load capacity of the structure at the elastic limit and corresponding to the displacement $\Delta_e$, Ω is the overstrength factor and β is the ratio of the factored gravity loads to the axial load presents during the design earthquake conditions. Figure (2) illustrates an example of the proposed graphs. The design procedure will begin with determining an intended (predetermined) structure's instability coefficient θ, or critical buckling load factor, λ. By choosing the target lateral displacement and calculating the system's natural period of vibration using Equation (1), the corresponding base shear needed to achieve this lateral displacement without inducing instability during an earthquake will be identified from the relevant graph. Subsequent steps will involve analyzing and designing the structure using the equivalent lateral load method in accordance with the design code's requirements.

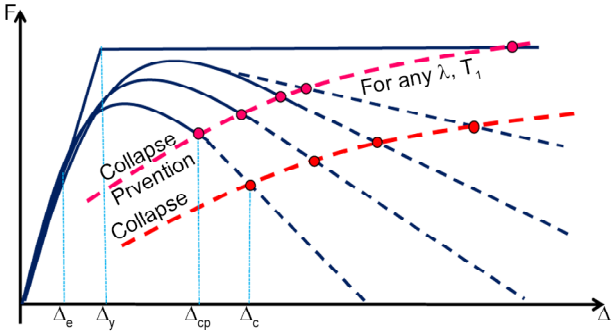


**Figure 2.** Stability based design of mass subsystem (Boujary & Ziyaeifar, 2019a-b).

In these studies, it was assumed that up to the design-based earthquake intensity levels (DBE), no contact occurs between the two parts. However, due to architectural considerations and the limitations in the isolation distance (gap) between the two subsystems, it is inevitable that the two substructures will collide during earthquakes with an intensity greater than the DBE. According to Figure (3), alterations in the system's geometry will lead to changes in the buckling mode and the collapse mechanism of the mass subsystem. This will affect the seismic behavior of the structure, causing a backup system to activate, resulting in multi-phase behavior within the system (Figure 4). Consequently, the design approach should be structured to utilize the capacity of the stiffness subsystem to ensure the stability of the mass subsystem.

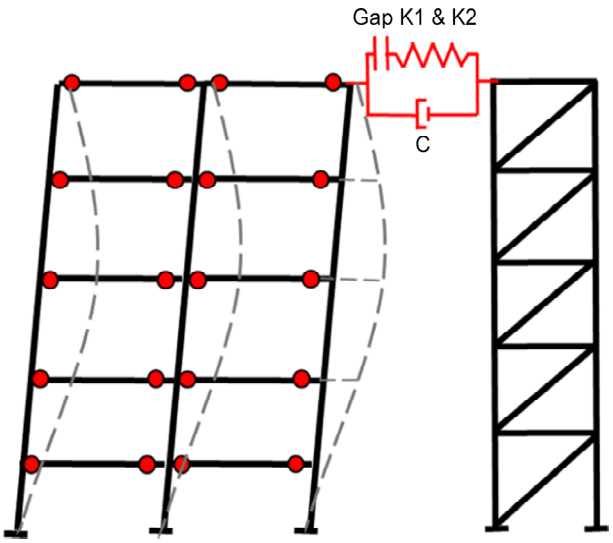


**Figure 3.** Subsystems' contact and change in buckling mode of mass subsystem (Saharkhizan & Ziyaeifar, 2024).

### *2.2. Expected Dollapse Behavior*

According to Figure (4), after connecting the two parts, the ductility, stiffness and strength capacity of the stiffness subsystem can be used to improve the stability of the mass subsystem (increase in the λ parameter). This condition is considered a significant advantage for mass-isolated structures, as for earthquake intensity exceeding the design level, the stiffness subsystem functions as a backup system, improves the displacement capacity of the mass subsystem and, consequently, enhances the overall performance of the system. This phenomenal effect decreases the possibility of system collapse while increasing the system's reliability in the event of a sever earthquake.

In this regard, attention must be given to reducing the stiffness of the subsystems by increasing the height of the structure and its adverse impact on the performance of the energy dissipation mechanism (softening of the stiffness subsystem behind the damper as a support). Additionally, the failure conditions of energy dissipation devices should be considered in design process. Consequently, the design of the stiffness subsystem will be based on achieving the maximum possible stiffness while securing an appropriate yielding mechanism based on the maximum transfer forces from the mass subsystem and damping instruments.

## 3. Nonlinear analysis (methodology)

The research methodology employed in this study relies on numerical simulation and nonlinear time history analysis, conducted in three stages as follows:

- Equivalent tow degrees of freedom (2-DOF) model for initial parametric studies
- Simplified cantiliver column model for impact mechanism modeling
- Real structural frame model for collapse mechanism investigation.

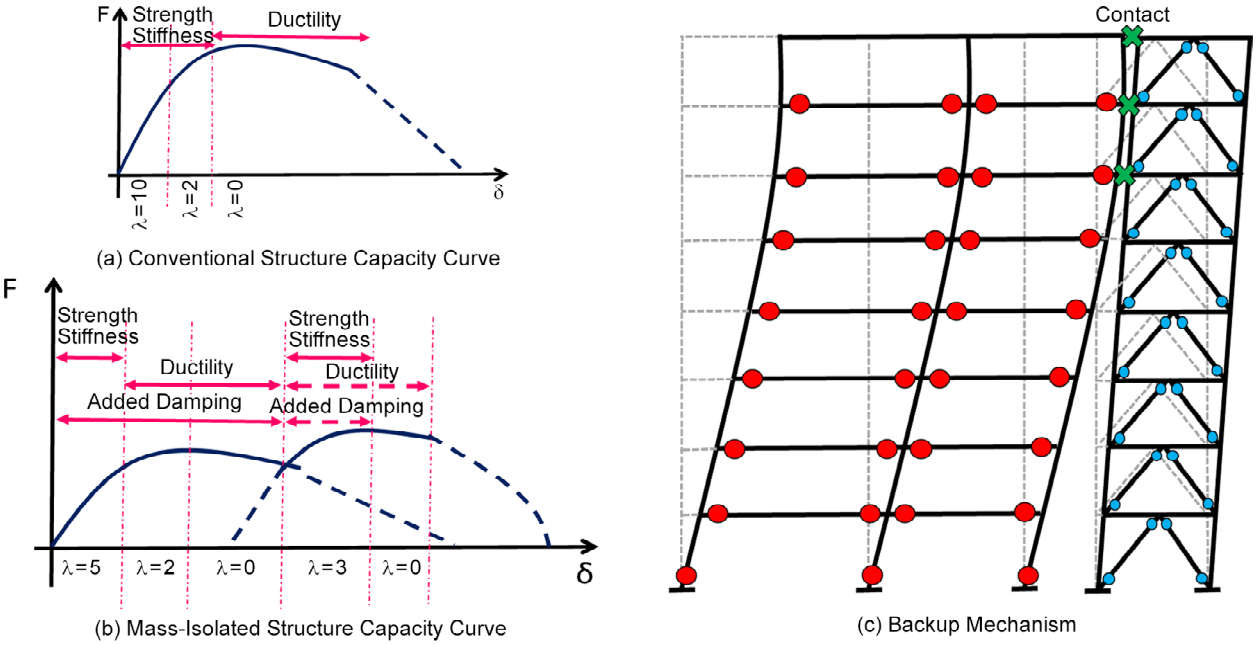


**Figure 4.** The effect of subsystems interaction on the collapse capacity (instability) of mass subsystem (Saharkhizan & Ziyaeifar, 2024).

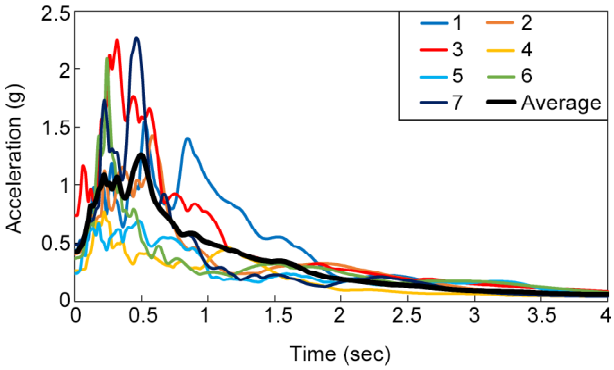


**Figure 5.** Response spectrum of selected ground motion records.

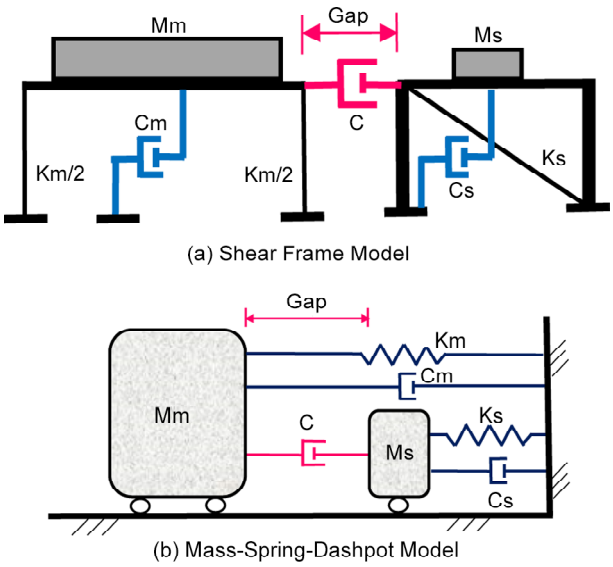


**Figure 6.** 2-DOF model.

For this porpose, seven far field ground motion records selected for nonlinear time history analysis with general characteristics are presented in Table (1), as well as the acceleration response spectrum of each, and the average of the records are illustrated in Figure (5).

## 4. Equivalent 2-DOF Analytical Model Approach

In order to investigate the nonlinear behavior of the mass isolated structure under seismic excitation, an equivalent two-degree-of-freedom (2-DOF) model has been developed. The shear frame and simplified mathematical model of this system is shown in Figures (6a) and (6b), respectively. The dynamic equations of motion governing the vibration of this system under external seismic excitation are presented in Equations (6) and (7). $M_m$, $C_m$ and $K_m$ are the mass, damping coefficient and stiffness of the mass subsystem and $M_s$, $C_s$ and $K_s$ are the mass, damping coefficient and stiffness of the stiffness subsystem, respectively. $C$ is the damping coefficient of viscose damper connecting two substructures, and $\ddot{u}_g$ is the input ground motion acceleration intensity. $\ddot{u}$, $\dot{u}$ and $u$ are the acceleration, velocity and displacement response of subsystems, respectively. The presented 2-DOF model, with a close estimation, can predict the seismic behavior of mass-isolated structures under real earthquake excitation with a much lower computational cost. Estimated equivalent dynamic property of subsystems presented in Table (2).

$$\begin{cases} M_m\ddot{u}_m + C_m\dot{u}_m + K_m u_m + C(\dot{u}_m - \dot{u}_s) = -M_m\ddot{u}_g & (6) \\ M_s\ddot{u}_s + C_s\dot{u}_s + K_s u_s - C(\dot{u}_m - \dot{u}_s) = -M_s\ddot{u}_g & (7) \end{cases}$$

**Table 1.** Ground motion records set for nonlinear time history analysis (FEMA P695).

| Number | Ground motion ID | Year | M | PGV(cm/s) | PGA (g) | Station |
|---|---|---|---|---|---|---|
| 1 | Northridge | 1994 | 6.7 | 63 | 0.44 | Beverly Hills - Mulhol |
| 2 | Northridge | 1994 | 6.7 | 45 | 0.40 | Canyon Country-WLC |
| 3 | Duzce, Turkey | 1999 | 7.1 | 62 | 0.74 | Bolu |
| 4 | Hector Mine | 1999 | 7.1 | 42 | 0.26 | Hector |
| 5 | Imperial Valley | 1979 | 6.5 | 33 | 0.23 | Delta |
| 6 | El Centro (Imperial Valley) | 1979 | 6.5 | 42 | 0.37 | El Centro Array #11 |
| 7 | Kobe, Japan | 1995 | 6.9 | 37 | 0.48 | Nishi-Akashi |

**Table 2.** Equivalent 2-DOF model's specification.

| Subsystem | M (kg) | K (N/m) | T (sec) | Fy (N) | Uy (m) | Damping Ratio ($\xi$) |
|---|---|---|---|---|---|---|
| **Mass** | 1.25e5 | 1.50e6 | 1.750 | 3.0e5 | 0.20 | 0.03 |
| **Stiffness** | 0.25e5 | 4.50e6 | 0.475 | 4.5e5 | 0.10 | 0.03 |
| **Ratio (M/S)** | 5 | 1/3 | 3.70 | 2/3 | 2 | 1 |

### 4.1. Damping Coefficient Estimation

The first step in seismic design procedure of this system is to choose appropriate and reasonable values for system damping coefficient. Figures (7a) to (7g) indicate the maximum displacement response of the system for different earthquake ground motion and Figure (7h) illustrates the average response for records ensemble. It should be mentioned that the algorithm used for these parametric nonlinear time history analysis' in MATLAB is based on the Newmark-β method with linear changes of acceleration, and the nonlinear

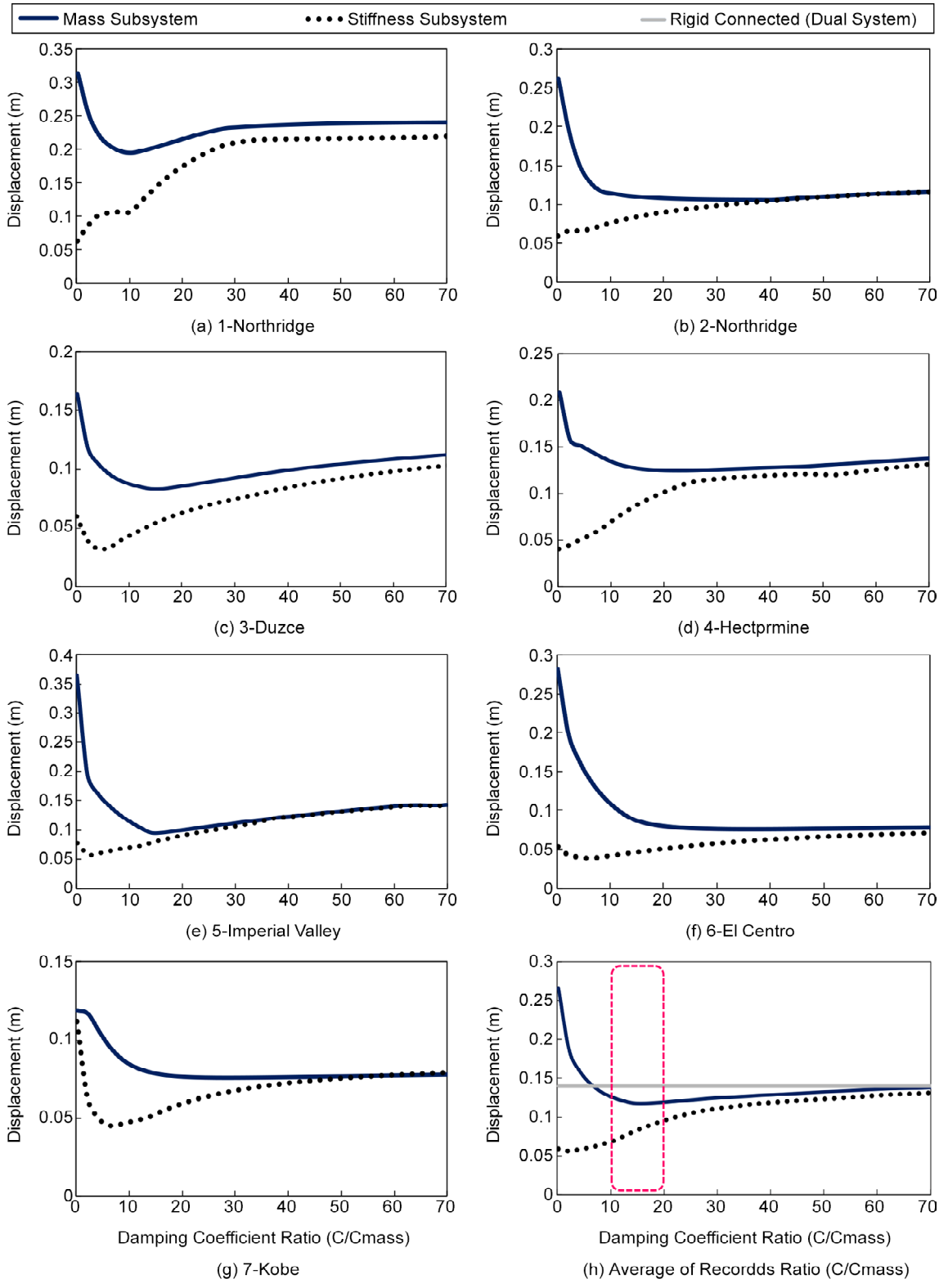


**Figure 7.** Maximum displacement response for variable damping coefficient.

behavior is assumed to be elastic-perfectly plastic (Chopra, 2021).

The overall trend of the maximum displacement response as the ratio of the damping coefficient ($C/C_{mass}$ for $C_{mass} = 2\xi M_{mass}\omega_{mass}$) increases across different phases is as follows: in the range of $(0 < C)/(C_{mass} < 5)$, a positive effect of increasing the damping is observed, as it reduces the maximum displacement response for both subsystems (notably, there is a sharp decrease in the response of the mass subsystem and a relative reduction in the stiffness subsystem's response). After that, for the range of $(5 < C)/(C_{mass} < 10)$, while the response of the mass subsystem continues to decline (with a reducing rate), the response of the stiffness subsystem begins to increase. For $(10 < C)/(C_{mass} < 20)$, the displacement response of the mass subsystem reaches its minimum value, while the response of the stiffness subsystem exhibits a decrease of approximately 50% compared to the scenario with a rigid connection. This area is identified as the optimal zone for damping coefficient ratio (where, while controlling the response of the mass subsystem as the primary component of the structure, a significant portion of the stiffness subsystem's capacity can be preserved for extremely severe earthquakes). As the damping increases further $(C/(C_{mass} > 20))$, the system's behavior approaches that of the original dual system (rigid connection) and the positive effect of the damper is eliminated.

### *4.2. Seismic Behavior*

In order to more accurately investigate the seismic behavior of the mass-isolated system, the displacement response and the hysteresis curve of the 2-DOF model under 6th ground motion record of Table (1) (El Centro - Imperial Valley) are presented in Figure (8) for the following three cases: 1. Isolated structure without damping, 2. Isolated structure with optimal damping ($C/(C_{mass} = 15)$), and 3. State of the rigidly connected subsystems are shown.

In case 1, regarding the philosophy of designing the softest possible structure for the mass subsystem, under strong earthquake excitation, the mass subsystem will exhibit significant displacement responses. This figure confirms that, to ensure the stability of the mass subsystem, a damping mechanism and a stiffness subsystem will definitely be needed as a backup system. For case 2, it is observed that the presence of damping alleviates the displacement of the mass subsystem, while limiting the behavior of the two parts to the elastic phase, effectively eliminating any residual displacement.

For case 3 (rigid connection), while the behavioral phase of the system changes from the initial yielding of the mass subsystem (similar to the second case) to the initial yielding of the stiffness subsystem (similar to the conventional dual system), the intensity of the nonlinear behavior in the system increases and the residual displacement in the system is observed. In this scenario, by the stiffness subsystem yielding at the DBE level, only the ductility capacity of the mass subsystem remains to ensure the collapse prevention performance level. This is while for the mass-isolated case, the capacity of the stiffness subsystem exists to prevent collapse in MCE level as an extra resource, and this phenomenon can increase the reliability of the structure in case of a severe earthquake respect to connected state.

## 5. Impact Model

To investigate the collapse behavior of the system, modeling the impact of two substructures (as described in section 2) will be crucial. in this regard, a force-based impact modeling approach was investigated (Hao et al., 2013; Miari et al., 2019).

According to Figure (9), to model the impact mechanism of the two subsystems, a combination of gap, hook, and dashpot elements has been utilized. A simple lumped mass two-degree-of-freedom cantilever column model with a frequency ratio of approximately 4 ($\omega_{stiff}/\omega_{mass} = T_{mass}/T_{stiff} \cong 4$) was developed and subjected to nonlinear time history analysis.

The gap (hook) distance between the two subsystems is set at 8 centimeters (approximately 1.25% drift for a story height of 6.4 meters), with additional structural properties outlined in Table (3). The Steel-01 material, featuring a yield stress of 240 MPa and a modulus of elasticity of 2e5 MPa, is employed for modeling material nonlinearity. Force-based nonlinear beam-column element based

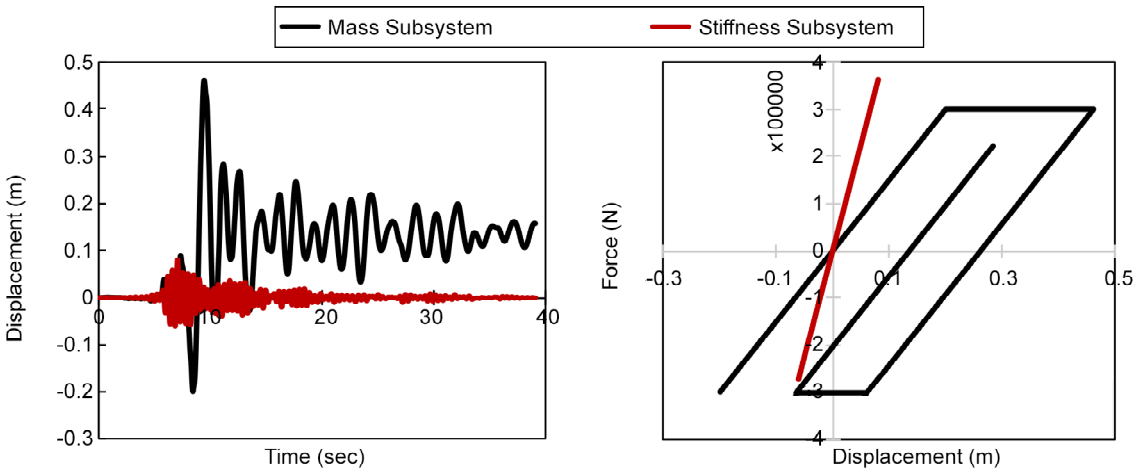


(a) Case 1: (Left) Displacement Response and (Right) Hysteresis Curve

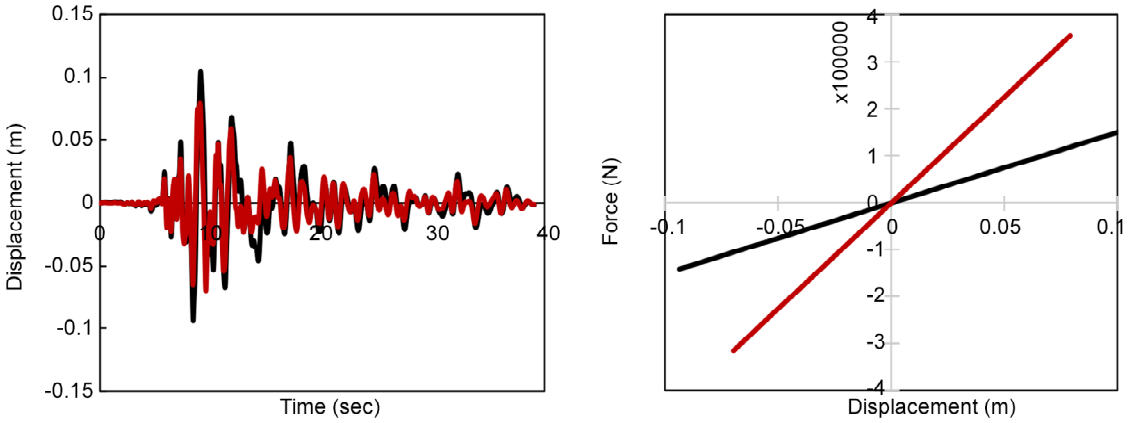


(b) Case 2: (Left) Displacement Response and (Right) Hysteresis Curve

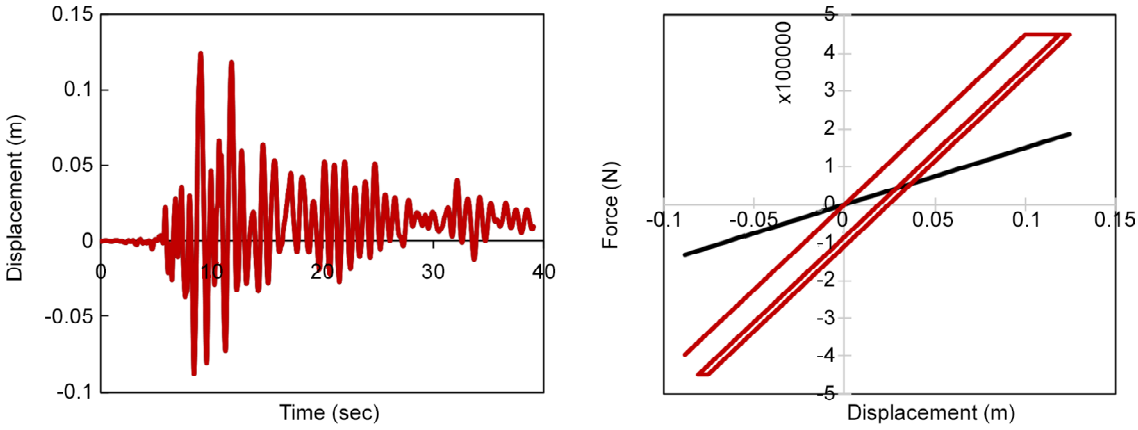


(c) Case 3: (Left) Displacement Response and (Right) Hysteresis Curve

**Figure 8.** Responses time history.

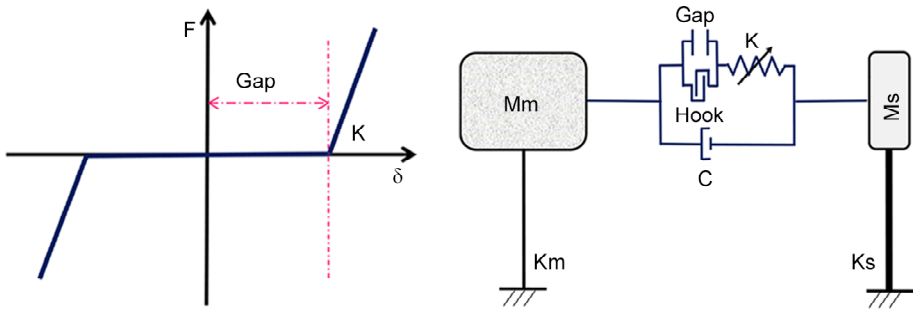


(a) Gap-Hook-Spring Mechanism (b) Cantilever Column Impact Model

**Figure 9.** Impact model.

on fiber formulation is utilized for structural components in Opensees (Mazzoni et al., 2005).

Figure (10a) illustrates the numbers and values of impacts between two subsystems under Northridge ground motion record (first record from Table 1) for the case of $C/(C_{mass} \cong 1)$. The impact, displacement,

**Table 3.** Structural property for cantilever column impact model.

| Subsystem | M (kg) | K (N/m) | T (sec) | I ($m^4$) | Z ($m^3$) | H (m) | Cross-section |
|---|---|---|---|---|---|---|---|
| Mass | 30000 | 1.25e6 | ~1.00 | 1.35e-4 | 1.05e-3 | 6.4 | C1* |
| Stiffness | 6000 | 3.65e6 | ~0.25 | 4.00e-4 | 2.50e-3 | 6.4 | C5* |

* Specification for cross-sections are presented ahead in Table (4).

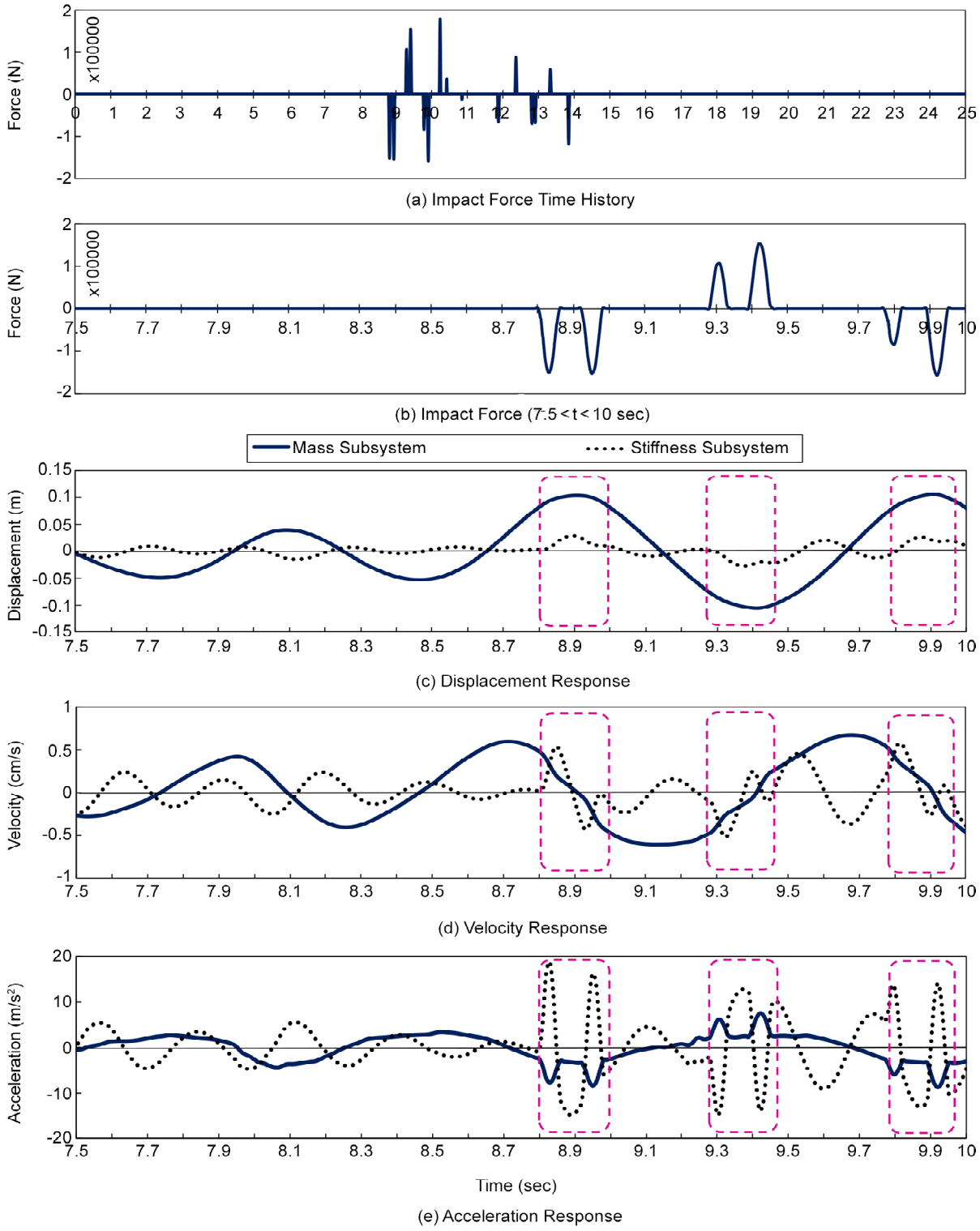


**Figure 10.** Impact response time histories.

velocity, and acceleration responses of the system during the time interval from 7.5 to 10 seconds (when six contacts occur) are depicted in Figures (10b) to (10e).

- According to the impact mechanism and response of subsystems, the following results can be deduced:
- Contact primarily occurs during the maximum displacement of the mass subsystem.
- Because substructure velocities are relatively low during contact, the collision of two parts does not result in a significant change in the momentum of the mass subsystem. However, the impact increases the velocity deceleration rate of the mass subsystem.
- Due to the small mass of the stiffness subsystem compared to the mass subsystem, the collision of two parts results in a substantial change in the momentum of the stiffness subsystem (velocity and acceleration increasing).
- Due to the subsystems being subjected to earthquake excitation, they can be influenced by the earthquake ground motion, experiencing rapid changes in velocity, acceleration, and displacement immediately following the impact. This phenomenon occurs particularly within the stiffness substructure.

The collision of two subsystems causes a change in the momentum of two parts. Depending on the velocity reduction rate and the change in the lateral displacement of the subsystems, this event can improve the stability of the system. In addition, this penomenon can enhance radiation damping in the system by exciting local modes and resulting in energy dissipation in the form of sound, heat, and friction.

Figure (11) illustrates the system's response to two distinct levels of earthquake intensity. It is evident that for the unscaled ground motion intensity (Figure 11a), the impacts were not ecessively severe, and the presence of damping in the system has considerably diminished the structure's responses. In contrast, for amplified ground motion (Figure 11b), the occurrence of severe collisions between two subsystems, in addition to intensifying the responses during the non-linear phase due to its shock nature, has resulted in considerable residual displacement, particularly in the stiffness subsystem.

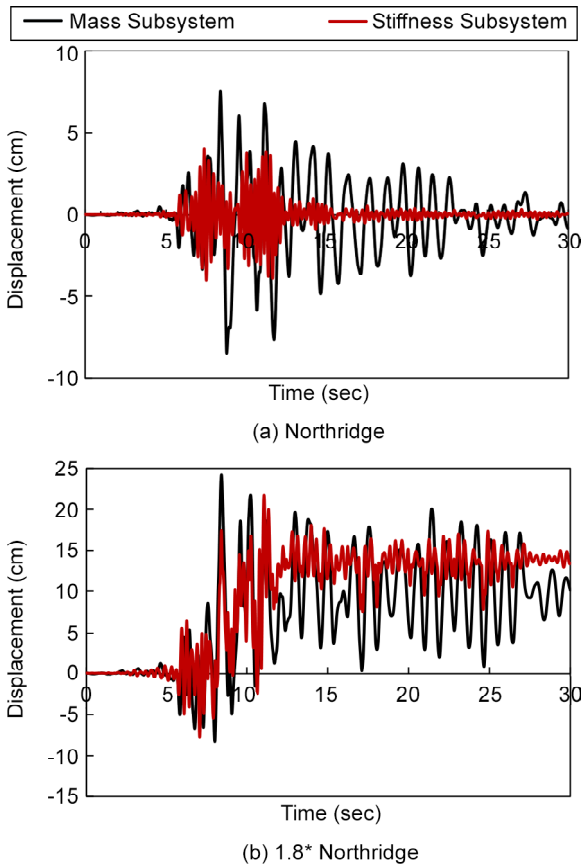


**Figure 11.** Impact response time history.

This issue can have substantial negative effects on the collapse prevention limit state and overal seismic performance of the system. Another critical problem is that, during the return of the mass subsystem to its initial position, the decrease in relative velocity and damping force leads to virtually no effective restoring force to mitigate the deformations of the stiffness subsystem and, consequently, to utilize the ductility capacity of this component. This matter needs to be carefully investigated to result in practical solutions in order to provide soft collision conditions (instead of rigid collision), such as the use of multi-stage damping mechanisms, which are being investigated by the authors.

## 6. Collapse Mechanism Investigation (Real Structural Frame Approach)

In this section, a two-dimensional five-story steel building frame (equivalent half 2D model of a real 3D mass-isolated structure) with a dual lateral load-bearing system (moment frame and concentric braced frame) designed as a case study according to the requirements of ASCE/SEI 7-21, AISC360-22

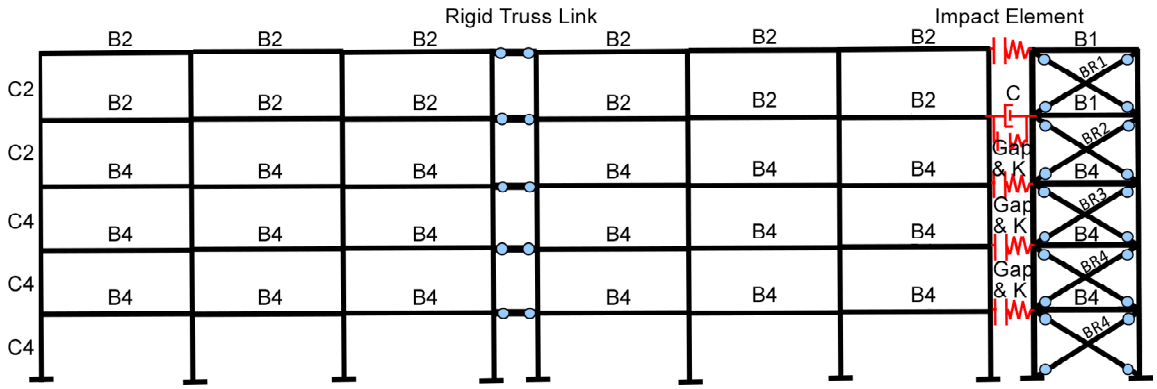


**Figure 12.** 5-story case study frame.

and AISC341-22 regulations without any special seismic design requirenment (in ordinary level) and then isolated (Figure 12) (ASCE/SEI 7, 2021, AISC360, 2022 and AISC341, 2022). Values of dead and live load are 24000 and 8000 N/m, respectively.

The span of all moment frames and braced frame are 6 and 5 meters, respectively, and the story height is 3.2 meters. The construction site is considered as class *D* and Rayleigh damping is considered with a damping ratio of 3%. Linear and nonlinear behavior adopted based on ASCE/SEI 41 requirements for steel material described in section 5 with seismically compact box and I-shaped cross-sections (ASCE/SEI 41, 2021). Nonlinear beam column element based on fiber formulation for beams and columns, and truss element with force displacement behavior modeled by hysteresis material for brace components are utilized in OpenSees.

Only one linear viscous damper was used in the fourth floor with the capacity of 5e5 N.s/m and to model the collision of two substructures in the stories, the impact model presented in section 5 was used. Other specifications of materials and cross-sections of structural components are presented in Figure (13) and Table (4).

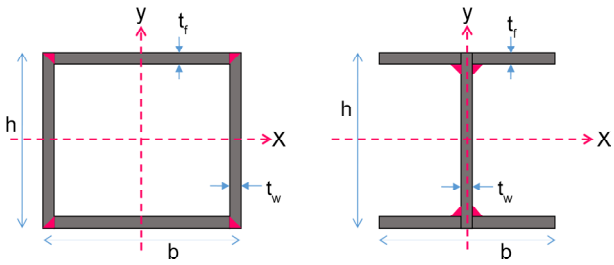


**Figure 13.** Cross-sections for beams, columns (right) and braces (left).

### *6.1. Static behavior*

Although the application of non-linear static analysis for this structural typology may not be entirely realistic, it offers valuable insights into the overall capacity of the mass-isolated structure, its seismic behavior, collapse mechanism, and performance variations compared to conventional structural systems.

According to the capacity curves presented in Figure (14), the following results can be inferred:

- The two-phase (stepping) behavior of the mass isolated system compared to the primary system.
- Increasing the lateral strength and stiffness of the mass subsystem after its connection to the stiffness substructure (enhancing seismic performance during larger lateral displacements).
- System's ductility enhancement by increasing

**Table 4.** Specifications of the cross-sections.

| Beam | | | | | Column | | | | | Brace | | | | |
|---|---|---|---|---|---|---|---|---|---|---|---|---|---|---|
| Section | *h* (mm) | *B* (mm) | $t_f$ (mm) | $t_w$ (mm) | Section | *h* (mm) | *B* (mm) | $t_f$ (mm) | $t_w$ (mm) | Section | *h* (mm) | *B* (mm) | $t_f$ (mm) | $t_w$ (mm) |
| **B1** | 200 | 100 | 8 | 6 | **C1** | 300 | 200 | 15 | 10 | **BR1** | 80 | 80 | 6 | 6 |
| **B2** | 220 | 100 | 8 | 6 | **C2** | 330 | 240 | 15 | 12 | **BR2** | 100 | 100 | 6 | 6 |
| **B3** | 240 | 120 | 10 | 8 | **C3** | 340 | 280 | 18 | 15 | **BR3** | 100 | 100 | 8 | 8 |
| **B4** | 280 | 160 | 10 | 8 | **C4** | 340 | 300 | 20 | 15 | **BR4** | 120 | 120 | 8 | 8 |
| **B5** | 300 | 180 | 12 | 8 | **C5** | 360 | 300 | 20 | 18 | **BR5** | 120 | 120 | 10 | 10 |

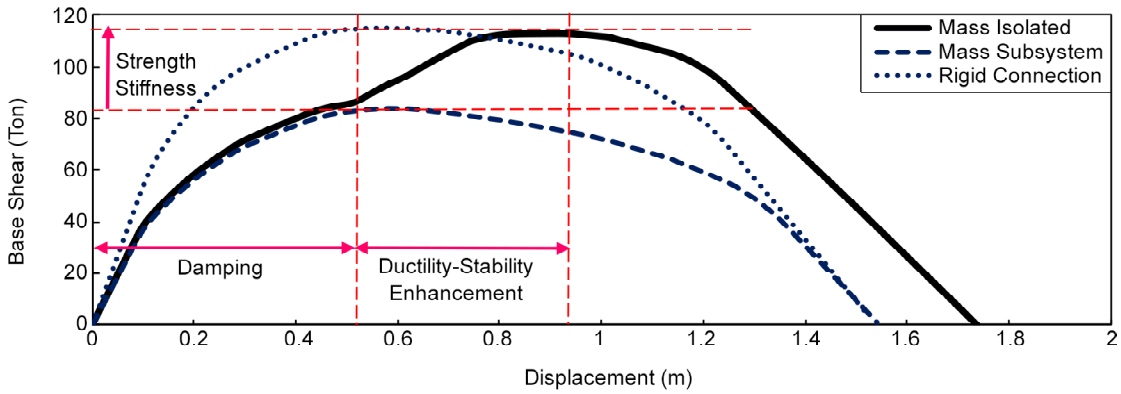


**Figure 14.** Capacity curve.

the value of lateral displacement equivalent to the system collapse limit state.

- Improving the system's stability by postponing the lateral collapse (resulting in a relative reduction of collapse probability).

### *6.2. Dynamic Behavior*

Figure (15) illustrates average values of maximum inter-story drift ratio (as a damage measure) of mass-isolated and dual 5-story case study frames versus incremental PGA values (as an intensity measure with steps of 0.2 g) for selected ground motion records. For ground motion intensity up to around PGA = 0.6 g, the presence of the viscouse damper in the fourth floor has been able to maintain the response of the mass subsystem around the maximum response of the dual system (rigidly connected) with a slight difference, while a significant portion of the stiffness subsystem's capacity remains untapped. For larger values of PGA, the response of the mass subsystem shows a relative increase compared to the connected state. Finally, the connected system undergoes dynamic instability at intensity of about PGA=1.4 g (a sharp increase in the response because of a slight change in the input earthquake intensity). This is while due to the existence of damping sources and the ductility capacity of the stiffness substructure, the intensity that causes dynamic instability in the mass-isolated structure increases to about PGA = 1.7 g.

The reason for this phenomenon is that, for moderate to severe earthquakes (DBE level), the strength, stiffness and ductility capacity of the mass subsystem and the damping capacity of connecting damper will provide the stability of this substructure. Besides, for higher intensity (MCE level), the mass subsystem connects to the stiffness subsystem after passing the gap between the two subsystems, and in this way, by changing its buckling mode, the stability of this part is ensured and until the stiffness subsystem reaches its collapse threshould, the mass subsystem will also be stable. In other words,

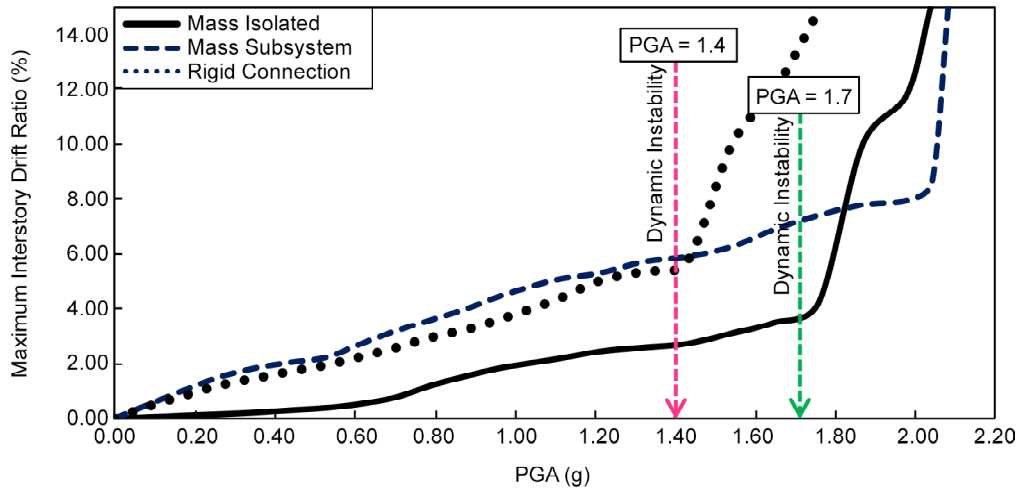


**Figure 15.** Incremental dynamic analysis response.

the collapse of the mass-isolated system is tightly controlled by the occurrence of instability in the stiffness subsystem, and it can be claimed that under input excitations, on average, the isolated structure shows about 21% higher collapse capacity than the connected structure state (dual system).

## 7. Conclusion

In this study, the collapse mechanism of mass-isolated systems and its seismic behavior differences compared to conventional dual systems were investigated. Results indicate that, it is possible to advance the collapse point of the mass subsystem to the collapse threshold of the stiffness subsystem, provided that no instability occurs in the mass subsystem until this limit state. It should be noted that before connecting the two parts, due to the significant increase in the damping capacity of the system (considerable relative displacement and velocity take place between two substructures), most of the earthquake input energy will be dissipated and, as a result, the seismic demand in the main structural components will be reduced. Achieving such a damping amplification mechanism and increased damping ratio is not feasible in the conventional code-compliant structural system. Additionally, employing structural configurations with multi-phase behavior that can utilize mechanisms and extra resources other than ductility for seismic intensity exceeding the DBE level to prevent global instability will be highly effective in reducing structural collapse probability. In other words, it can be claimed that to increase the reliability of structures during severe earthquakes, the philosophy of seismic design should shift from the design of conventional integrated structures to mass-isolated structural typology to provide a high damping ratio and reduce structural demand, damages, and consequently collapse probability.

## References

AISC (2022). *Specification for Structural Steel Buildings (ANSI/AISC 341-22), AISC Committee.*

AISC (2022). *Specification for Structural Steel Buildings (ANSI/AISC 360-22), AISC Committee.*

ASCE (2022, January). *Minimum Design Loads and Associated Criteria for Buildings and Other Structures*, *ASCE/SEI 7-22*. American Society of Civil Engineers. doi: 10.1061/9780784415788.

ASCE (2023). Seismic evaluation and retrofit of existing buildings, ASCE/SEI 41-23. *American Society of Civil Engineers*. doi: 10.1061/9780784416112.

Bernal, D. (1992). Instability of buildings subjected to earthquakes. *Journal of Structural Engineering-asce*, *118*(8), 2239-2260. doi: 10.1061/(asce)0733-9445(1992)118:8(2239.

Bernal, D. (1998). Instability of buildings during seismic response. *Engineering Structures*, *20*(4-6), 496-502. doi: 10.1016/s0141-0296(97)00037-0.

Boujary, M. & Ziyaeifar, M. (2019a). Design of mass isolated structures with consideration of stability constraints. *Journal of Seismology and Earthquake Engineering*, *21*(3), 49-63. http://www.jsee.ir/article_241708_677edba4dbe2c6cf0a252097f7299942.pdf.

Boujary, M. & Ziyaeifar, M. (2019b). Initial solution for designing a soft substructure in a mass isolation system with consideration of stability constraints. *Journal of Seismology and Earthquake Engineering*, *21*(4), 37-48. http://www.jsee.ir/article_243310_5d37b03c774412b98c27b7835958096e.pdf.

Cheng, F.Y., Jiang, H. & Lou, K. (2008). *Smart Structures: Innovative Systems for Seismic Response Control*. http://ci.nii.ac.jp/ncid/BA87270937.

Chopra, A.K. (2021). *Dynamics of Structures: Theory and Applications to Earthquake Engineering*, (5th ed.), Prentice-Hall, Englewood Cliffs, NJ.

Du, L., Zhang, W., Tu, Y., Song, S., Sas, G. & Elfgren, L. (2022). Shaking table test on a novel mega-frame suspended structural system. *Journal of Building Engineering*, *52*, 104440. doi: 10.1016/j.jobe.2022.104440.

FEMA (2009). *Quantification of Seismic Performance Factors, FEMA P-695 Report, Prepared by the Applied Technology Council for the Federal Emergency Management Agency*, Washington, DC.

Hao, H., Bi, K., Chouw, N., & Ren, W.X. (2013).

State-of-the-art review on seismic induced pounding response of bridge structures. *Journal of Earthquake and Tsunami*, *7*(03), 1350019.

Maleki, A., Khalili Sarbangoli, R, & K. Badri, R. (2024). Evaluation of cyclic behavior of steel frame with infill plate and eccentric brace. *9th International Conference on Seismology and Earthquake Engineering*, Tehran, Iran.

Mazzoni, F., McKenna, S., Fenves, G.L. (2005). *OpenSees Command Language Manual*. Pacific Earthq. Eng. Res. Cent. 264.

Miari, M., Choong, K.K., & Jankowski, R. (2019). Seismic pounding between adjacent buildings: Identification of parameters, soil interaction issues and mitigation measures. *Soil Dynamics and Earthquake Engineering*, *121*, 135-150.

Nakamura, Y., Saruta, M., Wada, A., Takeuchi, T., Hikone, S. & Takahashi, T. (2010). Development of the core-suspended isolation system. *Earthquake Engineering & Structural Dynamics*, *40*(4), 429-447. doi: 10.1002/eqe.1036.

PEER (2017). *Guidelines for Performance-Based Seismic Design of Tall Buildings*. Pacific Earthquake Engineering Research Center

Saharkhizan, S. & Ziyaeifar, M. (2024). Seismic design of structural system with multi-phase behavior. *9th International Conference on Seismology and Earthquake Engineering*, SEE9-00260012p.

Ye, Z., Feng, D. & Wu, G. (2019). Seismic control of modularized suspended structures with optimal vertical distributions of the secondary structure parameters. *Engineering Structures*, *183*, 160-179. doi: 10.1016/j.engstruct.2018.12.099.

Ziaeifar, M. (2002). Mass isolation, concept and techniques. *Journal of European Association of Earthquake Engineering*, *2*, 43-55. http://en.journals.sid.ir/ViewPaper.aspx?ID=69007.

Ziyaeifar, M., Gidfar, S. & Nekooei, M. (2011). A model for Mass Isolation study in seismic design of structures. *Structural Control & Health Monitoring*, *19*(6), 627-645. doi: 10.1002/stc.459